Influence of the Rigidity of a Provisional Restoration Supported on Four Immediately Loaded Implants in the Edentulous Maxilla on Biomechanical Bone-Implant Interactions Under Simulated Bruxism Conditions: A Three-Dimensional Finite Element Analysis

Kikue Yamaguchi, DDS[a]/Yuichi Ishiura, DDS, PhD[b]/Shinpei Tanaka, DDS, PhD[c]/Kazuyoshi Baba, DDS, PhD[d]

Purpose: The aims of this study were to *(1)* establish a biomechanical model that simulates the full-arch restoration supported by immediately loaded implants, which is customized for individual patients, and *(2)* clarify the effect of the implant placement and rigidity of a provisional restoration on the biomechanical response at the bone-implant interface. ***Materials and Methods:*** Three-dimensional finite element analysis models of a maxillary full-arch prosthesis supported by four immediately loaded implants were created from computed tomography data of maxillary edentulous patients. Displacements of the implants and equivalent stress on the bone around the implants under the loading conditions that simulated sleep bruxism were then calculated for these models. The effects of the implant placement angle (vertical or inclined), the reinforcement of the provisional restoration (with or without reinforcement), and the implant length on the maximum displacements of each implant were investigated, in addition to the average equivalent stress of the bone around the implant. ***Results:*** A longer implant and rigid restoration with reinforcement have the potential to reduce implant displacements and associated bone stress; however, the rigidity of the restoration had a much more significant effect on these parameters. ***Conclusions:*** The rigidity of full-arch provisional restorations supported by four immediately loaded implants should be improved by reinforcements, which could ensure the successful achievement of osseointegration by reducing load-induced micromovements of the implants. *Int J Prosthodont 2014;27:442–450. doi: 10.11607/ijp.3857*

Conventional implant protocols require a load-free healing period of 3 to 6 months between placement and functional loading of the implants.[1–4] Many efforts have been made to minimize the duration of the treatment period, and several reports have documented immediate loading protocols that enable immediate function with a provisional or definitive prosthesis after placement.[5–11] Merits of these protocols include a shortened treatment period, which enables early recovery of function, and the preservation of soft tissue architecture when the implants are placed immediately after tooth extraction.[12]

Micromovements of Immediately Loaded Implants

In the maxilla, the dominant bone type is trabecular bone, and the thin layer of cortical bone can make it difficult to achieve primary implant stability, which is an important parameter for successful osseointegration.[13] Several studies report lower implant success rates in the maxilla than in the mandible, which often has a higher proportion of cortical bone.[14] Therefore, maxillary full-arch restorations supported by immediately loaded implants are a challenge in patients with parafunctional activity, such as bruxism, because load-induced micromovements of implants during the initial healing period have the potential to disturb the process of osseointegration.[15]

[a]Postgraduate Student, Showa University School of Dentistry, Department of Prosthodontics, Tokyo, Japan.
[b]Assistant Professor, Showa University School of Dentistry, Department of Implant Dentistry, Tokyo, Japan.
[c]Assistant Professor, Showa University School of Dentistry, Department of Prosthodontics, Tokyo, Japan.
[d]Professor and Chair, Department of Prosthodontics, Showa University School of Dentistry, Tokyo, Japan.

Correspondence to: *Kazuyoshi Baba, DDS, PhD, Department of Prosthodontics, Showa University School of Dentistry, 2-1-1, Kita-senzoku, Ohta-ku, Tokyo 145-8515, Japan. Email: kazuyoshi@dent.showa-u.ac.jp*

Brunski et al[16] have suggested that immediate loading or early loading should be utilized only when micromovements are controlled below 100 μm. A large oscillation of the implant may not only disturb the attachment of the bone and implant but also lead to ingrowth of the soft tissue. Cameron et al[17,18] have reported that oscillations beyond 200 μm may produce contact between the connective tissue and the implant body, but that micromovements within 30 μm may not affect normal remodeling of the bone after surgery. Although these in vivo studies used mongrel dogs, they suggest that suppressing the micromovements of the implant is important for the successful achievement of osseointegration.[19–21]

Implant Placement and Rigidity of the Provisional Restoration Can Affect the Amplitude of the Micromovement

For controlling micromovements, several strategies are applicable in a clinical setting, depending upon the assumed influential factors, which include the type and number of implants to be placed and the design of the suprastructure.[22] Although a number of studies have reported on the biomechanical effect of the implant placement strategy on the bone-implant interface,[23–26] little is known about the effect of the suprastructure design, with the exception that the cantilever design should likely be avoided.[27,28] In the removable partial denture prosthodontic literature, however, rigid major connectors have been well documented to distribute the occlusal forces across the dental arch. This distribution of occlusal forces avoids load concentration on the abutment, where the direct retainer is placed.[29–32] The biomechanical behavior of tooth-supported removable partial dentures and that of implant-supported full fixed prostheses are different; however, these reports indirectly suggest that a rigid provisional restoration has the potential to decrease the load on the implant, which will then reduce the micromovements.

Prediction of Micromovement in Simulated Models

Three-dimensional (3D) finite element analysis (FEA) studies have been conducted to predict the micromovement of implants and associated bone stress under simulated loading conditions.[33,34] However, these studies generally used a predetermined uniform elastic modulus for creation of a simulated bone structure, which does not precisely reflect the biomechanical situation. Furthermore, in these FEA models, the implant surfaces were connected to the bone and did not, therefore, simulate an immediately loaded condition. The aims of this study were to *(1)* establish a biomechanical model that simulates the immediately loaded condition, which is customized for the individual patient, and *(2)* clarify the effect of the implant placement and rigidity of a provisional restoration on the biomechanical response at the bone-implant interface. To accomplish these aims, the authors constructed a 3D FEA model that simulated a full-arch provisional restoration supported by four dental implants placed in an edentulous maxilla. These models were created using the computed tomography (CT) data of patients to simulate not only bone morphology but also bone density, with the bone-implant surface contacts unconnected. Using this model, the authors investigated the displacements of the implants and bone stress around the implants under a loading condition that simulated sleep bruxism.

Materials and Methods

Edentulous Maxillary Bone Model

The CT images were acquired from three male patients (patient 1: 61 years; patient 2: 64 years; patient 3: 71 years) who were scheduled to receive implant treatment for an edentulous maxilla (HiSpeed QX/i, GE Healthcare) under the following conditions: tube voltage: 140 kV; tube current: 80 mA; slice thickness: 0.625 mm. The CT images were stored in a digital imaging and communications in medicine (DICOM) format. The bone morphology model of the edentulous maxilla for each patient was created from the DICOM data using computer software programs (Mechanical Finder [MF], Research Center of Computational Mechanics; and Rapidform XOR, 3D Systems). The CT data were handled anonymously, with appropriate ethical considerations. The study was fully explained to each participant, and consent was obtained for the use of the CT data. The study protocol was approved by the Ethics Committees of Showa University (no. 2011-12, July 27, 2011).

Implant and Provisional Restoration Models

Three-dimensional images of the implant complex, which consisted of the implant body, abutment, and temporary cylinder, were acquired by micro-CT (inspeXio SMX-90CT, Shimadzu) and stored in TIFF files. For each maxillary bone model, the implants were placed in four regions: the lateral incisors and second premolars on both sides. In terms of the implant placement, four vertical implants, including two vertical mesial implants and two inclined distal implants, were simulated. For the distal implants, five different lengths (10, 11.5, 13, 15, and 18 mm) of 4.0-mm–diameter

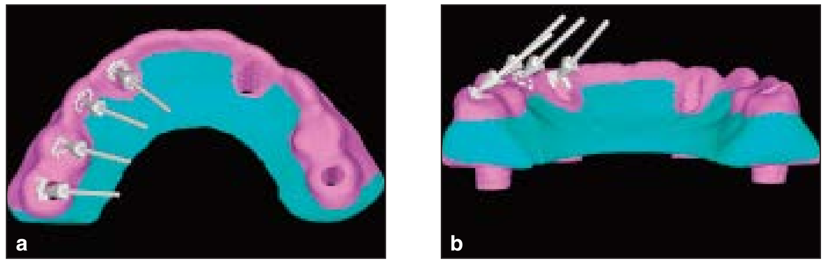

Fig 1 Reinforced provisional restoration under loading conditions (patient 3), with loaded nodes *(white dots)* and loading direction (white arrows) shown. The amplitudes of the applied loads were 42.4 N for the maxillary right lateral incisor, 45.4 N for the canine, 62.5 N for the first premolar, and 273.4 N for the second premolar. Pink color represents acrylic resin and blue color represents Co-Cr, which replaces palatal portion of the acrylic provisional restoration, excluding the portions of the artificial teeth and temporary cylinders: **(a)** occlusal view; **(b)** distal view.

Table 1 Implant Parts Used in This Study*

Implant body	Brånemark system Mk III RP, diameter 4.0 mm
Abutment	Multi-unit abutment, 1 mm Multi-unit abutment, 30 degrees, 4 mm
Temporary cylinder	Temporary abutment, titanium, nonengaging

*Nobel Biocare.

Table 2 Material Properties Used in This Study

Part	Material	Young's modulus*	Poisson's ratio
Reinforcement	Co-Cr	218 GPa†	0.3†
Provisional restoration	Acrylic resin	3.73 GPa‡	0.4‡
Implant complex	Titanium	105.91 GPa‡	0.19‡
Maxillary	Bone	—*	0.4‡

*Young's modulus of bone set for each element from the Hounsfield unit of the CT scan.
†Properties were taken from the literature.[35]
‡These values referred to preset data in the Mechanical Finder.

implants were simulated. In one patient, the inclined distal 18-mm–length implant was not simulated because sufficient bone volume was not available. The implant bodies, abutments, and implant angles simulated are summarized in Table 1.

Two acrylic provisional restoration models, with and without cobalt-chromium (Co-Cr) alloy reinforcement 0.5 mm in thickness, were created by editing the DICOM data of a radiographic guide and were connected to the implant complex model for each patient (Rapidform XOR; Fig 1). Overall, two implant placement angles, five implant lengths, and two types of provisional restorations were simulated.

FEA Model

All materials were considered homogeneous, isotropic, and linearly elastic except for the maxillary bone. The implants were made of titanium grade IV, and the provisional restorations were made of acrylic resin and Co-Cr. Material properties were taken from the literature, as shown in Table 2.[35] For the maxillary bone, the Young's modulus for each node was calculated from the Hounsfield unit of the CT data of each participant.[36,37] For simulating the immediate loading condition, the contact element for the interfacial condition was chosen between the bone and implant body with a coefficient of friction of 0.33.[38] The minimum mesh size of the analysis model was set at 0.2 mm for expressing the implant shape clearly and for conducting the analyses smoothly. The number of nodes was approximately 333,500 to 627,000, and the number of solid elements was approximately 1,634,000 to 3,094,000.

Loading Condition and Outcome Variables

For simulating parafunctional activity, the occlusal force during forceful grinding was measured from a patient with sleep bruxism (see Fig 1) using pressure-sensitive film (Dental Prescale, GC), and the measured force was applied against the palatal surface of the maxillary right lateral incisor and canine and the palatal incline of the buccal cusp of the maxillary right first and second premolars vertically (see Fig 1). All models were fully constrained in all directions at the nodes on the upper part of the sinus cavity.

Displacements of the implants and equivalent stress on the bone around the implants under the loading condition were calculated for these models. The effects of the implant placement angle (vertical or inclined), the reinforcement of the provisional

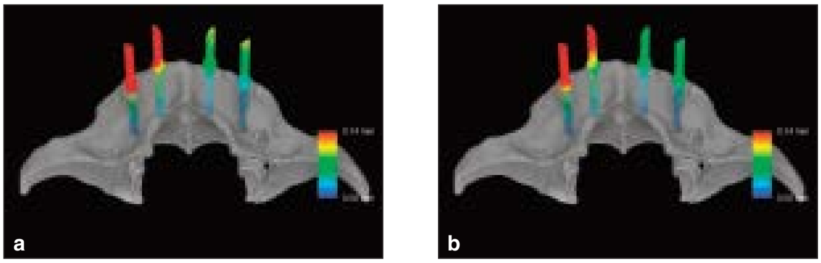

Fig 2 Examples of displacement of the implants on a contour map: **(a)** without reinforcement; **(b)** with reinforcement.

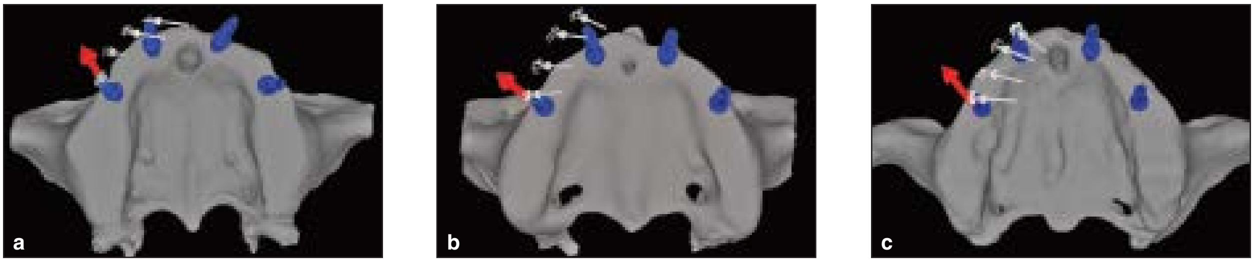

Fig 3 Displacement direction of the second premolar implant without reinforcement *(red arrow)* and loading direction *(white arrows)*: **(a)** patient 1; **(b)** patient 2; **(c)** patient 3.

restoration (with or without reinforcement), and the implant length on the maximum displacements of each implant were investigated. In addition, the average equivalent stress of the bone in a 10 mm (width) × 10 mm (depth) × 5 mm (height) rectangular solid platform was examined for each implant body, as well as the minimum and maximum principal strain and the average equivalent stress of the provisional restorations on the implant body.

Results

The displacements of the four implants under a simulated loading condition are shown in Fig 1. The amplitude of the displacements differed according to the individual; however, the largest displacement was consistently observed with the right second premolar implant body at the simulated cortical bone level (Fig 2) and was primarily directed toward the anterolateral direction (Fig 3). This trend was independent of the simulated conditions. Thus, the maximum amplitudes of the right second premolar implant displacements were analyzed exclusively.

For the second premolar implant, the longer implant was associated with a smaller displacement, with a single exception (patient 3, reinforced, vertical, 15 mm vs 18 mm). This trend was found to be independent of the placement angle, reinforcement, and the individual. The average difference in the displacement amplitude between the 10- and 18-mm implants was 5.7 ± 4.4 μm (4.7% ± 3.5% reduction of 18-mm implant), ranging from 0 μm to 15.19 μm. Regarding the effect of the angle, no consistent trend was found in this study.

The reinforcement of the provisional restoration reduced the displacement amplitude significantly and consistently, independent of the implant length, angle, or the person. The average reduction amplitude for all conditions was 37.2 ± 7.4 μm (27.2% ± 4.8% reduction), ranging from 26.9 μm to 48.2 μm, which was approximately 6.8 times as high as the effect of the length (Fig 4).

Equivalent Stress on the Bone Around the Implants

The distribution of equivalent stress on the bone around the four peri-implant sites is shown in Fig 5. The amplitude of the average equivalent stress on the bone was consistently found around the right second premolar implant. A stress concentration on the maxillary right anterior region also was observed.

Regarding the effect of implant length, the longer implants were associated with lower equivalent stress. This trend was found to be independent of the placement angle, reinforcement, or the individual. However, the effect of the implant angle was not consistent. Meanwhile, when the provisional restoration was reinforced, the stress level decreased around the right second premolar implant and increased around the left seond premolar implant. As a result, a better cross-arch force distribution was achieved when compared to the model without reinforcement (Fig 6). This trend was found consistently and was independent of the type of implant or the individual.

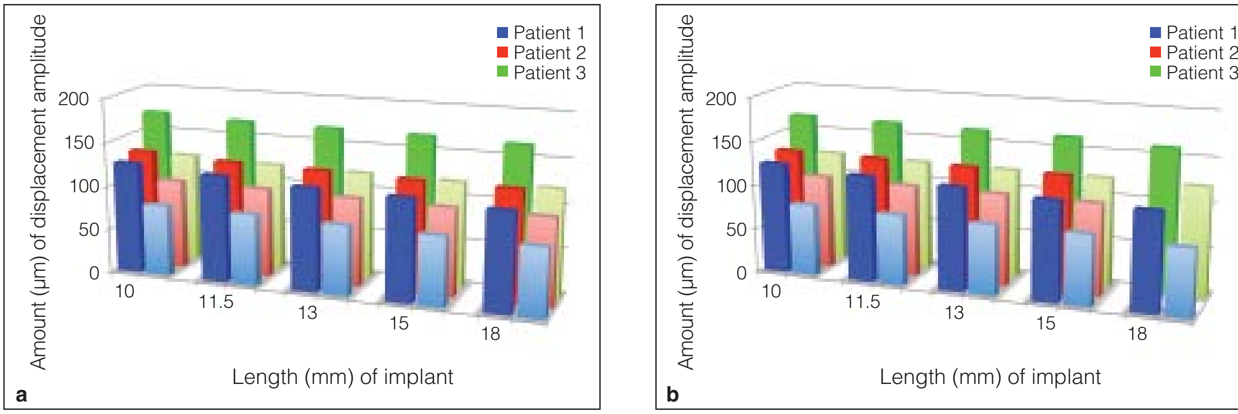

Fig 4 Maximum displacement of the right second premolar implant: **(a)** straight distal implant model; **(b)** inclined distal implant model. Inclined distal 18-mm implant was not simulated for patient 2 due to insufficient bone volume. Dark color bars (left 3 bars) = without reinforcement; light color bars (right 3 bars) = with reinforcement.

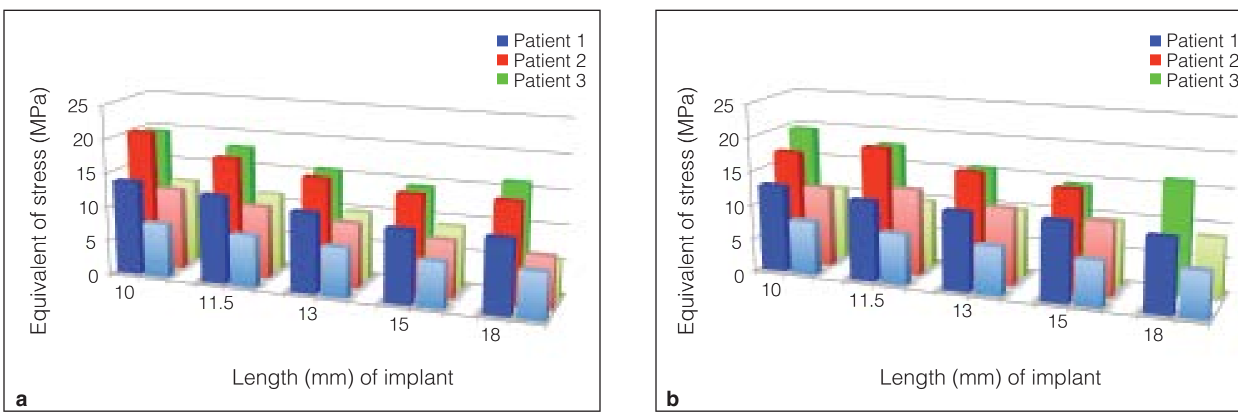

Fig 5 Maximum equivalent stress around the right second premolar implant: **(a)** straight distal implant model; **(b)** inclined distal implant model. Inclined distal 18-mm implant was not simulated for patient 2 due to insufficient bone volume. Dark color bars (left 3 bars) = without reinforcement; light color bars (right 3 bars) = with reinforcement.

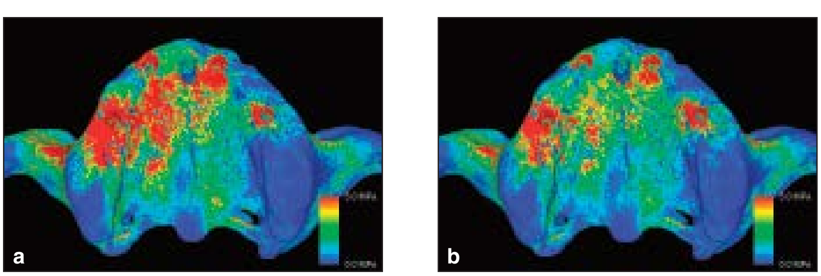

Fig 6 Equivalent stress distribution of the bone in a contour map: **(a)** without reinforcement; **(b)** with reinforcement.

Strain and Equivalent Stress on the Provisional Restorations

When force was applied, the provisional restoration was bent in a manner as shown in Fig 7. The maximum principal strains were reduced by the reinforcement (Fig 8; Table 3). The pattern of equivalent stress on the provisional restoration was generally in agreement with those on the bone around the implants. While the stress on the provisional restoration at the four implant sites, as evaluated by the contours, tended to distribute predominantly at the right second premolar implant region of the provisional restoration without reinforcement, a decrease in the stress at the right second premolar implant region and an increase at the left second premolar implant region were found when the provisional restoration was reinforced (Fig 9; Table 4). The effect of the implant length and inclination was not significant.

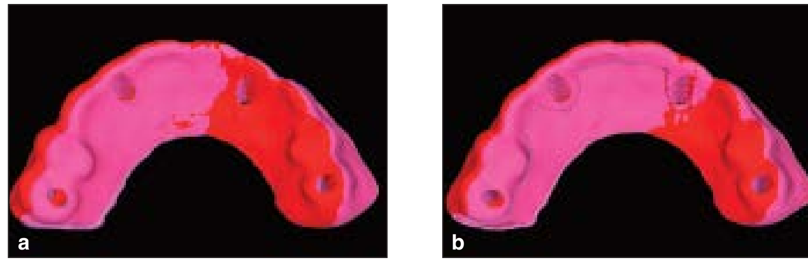

Fig 7 Deformation of the provisional restorations (patient 3). Pink color shows original position; red color shows deformed position deformation display in 3× magnification: **(a)** without reinforcement; **(b)** with reinforcement.

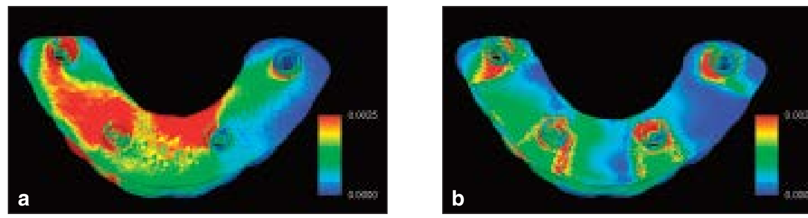

Fig 8 Maximum principal strain of the restoration at implant site in a contour map (patient 3): **(a)** without reinforcement; **(b)** with reinforcement.

Table 3 Maximum Principal Strain of the Restoration at Implant Site

	Straight distal implant model		Inclined distal implant model	
Implant length	Without reinforcement	With reinforcement	Without reinforcement	With reinforcement
Patient 1				
10 mm	0.4512	0.0356	0.0661	0.0701
11.5 mm	0.0403	0.0636	0.0509	0.0719
13 mm	0.2658	0.0370	0.0555	0.0560
15 mm	0.0606	0.0586	0.0678	0.0526
18 mm	0.0388	0.0618	0.0487	0.0569
Patient 2				
10 mm	0.1083	0.060	0.1164	0.1666
11.5 mm	0.049	0.0601	0.0663	0.0638
13 mm	0.1523	0.0504	0.072	0.0662
15 mm	0.0504	0.0410	0.0699	0.0735
18 mm	0.0469	0.0994	—*	—*
Patient 3				
10 mm	0.1236	0.0646	0.0584	0.0591
11.5 mm	0.064	0.0556	0.0788	0.0616
13 mm	0.0585	0.0550	0.0619	0.0613
15 mm	0.0944	0.0948	0.0694	0.0850
18 mm	0.0539	0.0690	0.0539	0.0636

*Inclined distal 18-mm implant was not simulated for patient 2 due to insufficient bone volume.

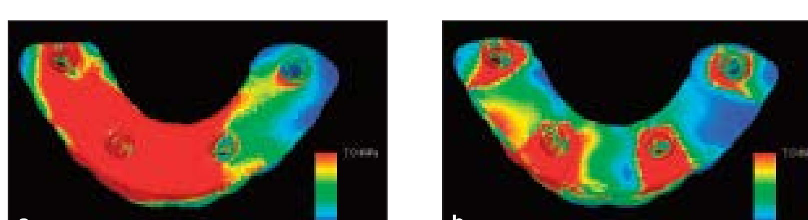

Fig 9 Equivalent stress of the restoration at implant site (patient 3): **(a)** without reinforcement; **(b)** with reinforcement.

Table 4 Maximum Equivalent Stress of the Restoration (MPa)

	Straight distal implant model		Inclined distal implant model	
Implant length	Without reinforcement	With reinforcement	Without reinforcement	With reinforcement
Patient 1				
10 mm	231.3	191.7	292.5	320.8
11.5 mm	173.8	173.8	238.4	373.8
13 mm	156.9	156.9	225.8	222.8
15 mm	259.2	259.2	213.3	260.6
18 mm	173.3	173.3	206.1	230.9
Patient 2				
10 mm	392.4	311.7	366.6	623.3
11.5 mm	303.5	285.1	340.6	290.9
13 mm	847.1	332.5	248.4	355.3
15 mm	347.4	298.6	407.2	430.3
18 mm	256.0	433.7	–*	–*
Patient 3				
10 mm	461.1	253.4	228.2	172.4
11.5 mm	214.4	225.4	320.2	307.8
13 mm	172.0	271.2	237.8	294.1
15 mm	394.9	341.6	232.0	364.0
18 mm	183.9	240.6	190.7	195.9

*Inclined distal 18-mm implant was not simulated for patient 2 due to insufficient bone volume.

Discussion

FEA Model

Biomechanical simulation, in which parafunctional loading was assumed to occur under an immediately loaded implant placement condition, was performed using 3D FEA models, which were created from the CT data of four maxillary edentulous patients. The advantage of this method was not only the precise simulation of bone morphology but also of Young's modulus, as determined by the Hounsfield units of the CT data.[37,39] This latter aspect is a clear advantage over previous simulations, which used predetermined equalized data.[40] That is, the simulation in the present study reflects not only bone morphology but also bone density, allowing for more precise biomechanical simulation under loading. Another advantage of the FEA models in the present study was the simulation of an immediately loaded condition by using the contact element between the bone and implant body. This condition enabled implant bodies to move certain amounts when the load was applied and is different from the connected condition, which should be regarded as a simulation of acquired osseointegration. To the authors' collective knowledge, no previous study has successfully simulated an immediately loaded condition using a method like the one reported here. In the future, individual and precise simulations should be conducted not only for research purposes but also in clinical settings to predict the biomechanical situation after implant placement. This study may promote such future efforts.

Study Results

The most remarkable finding of this study was that the rigidity of the provisional restoration showed the greatest impact on implant micromovement during simulated parafunction. In the literature, controlling the amplitude of implant micromovements and avoiding excessive stress at the bone-implant surface have been well documented to be necessary for the successful achievement of osseointegration.[15,17,18,23,41–43]

In the present simulation models, the nonrigid acrylic allowed for a large amount of bending and resulted in significant implant movement, which was associated with higher bone stress at the site of load application. When the restoration was reinforced, the maximum implant micromovement and stress at the bone under the loaded site decreased. Theoretically, rigid frameworks allow better distribution of occlusal forces by transmitting the force from the working side to the nonworking one across the dental arch.

For example, studies that investigated the effect of the rigidity of the major connectors of removable partial dentures on occlusal force distribution suggested a rigid connection allows for a better force distribution across the dental arch,[29,31] while the biomechanical behaviors of tooth-supported removable partial dentures and implant-supported fixed dentures are different. The current study demonstrated not only a decrease in stress on both the provisional restoration and peri-implant bone, but also an increase in these stresses at the opposite site (nonloaded side) of the dental arch, suggesting a better force distribution on the provisional restoration.

In both the literature and clinical settings, the length and diameter of the implant are reported to be significant factors for implant displacements and associated bone stress.[26] This study also observed the same trend, wherein a longer implant was associated with a smaller implant displacement and lower peri-implant bone stress. However, such an effect was much smaller than that of the reinforcement of the provisional restoration.

Clinical Implications

The preoperative planning and designing of implant placement based on bone morphology and mass by CT scans are essential for achieving safe, reliable implant placement and favorable outcomes. However, although this procedure has become routine, the evaluation and investigation of the biomechanical factor, which is an important component of implant treatment, is lacking. Thus, a preoperative plan and design should not only meet anatomical and morphological conditions but also reflect the functional loaded condition. The present study should be regarded as the first step toward creating such biomechanical simulations for implant treatment planning.

The finding that a rigid provisional restoration has the potential to reduce the amplitude of implant displacement during simulated loading conditions suggests that when full-arch provisional restorations supported by immediately loaded implants are planned, not only implant placement but also the materials used for restoration should be carefully selected from the viewpoint of the mechanical properties. That is, acrylic resin provisional restorations, which are commonly selected, should be reinforced by rigid material, such as a Co-Cr alloy, as simulated by this study, which may by effective for the successful achievement of osseointegration.

Lastly, it should be noted that other factors that potentially affect implant displacement, such as prosthesis designs, have not been investigated in this study, which is regarded as one of the study limitations. More comprehensive studies that include other significant factors should be conducted in the future to better understand the biomechanics of immediately loaded implant treatment.

Conclusions

The 3D FEA models of a maxillary full-arch prosthesis supported by four immediately loaded implants were created from CT data of maxillary edentulous patients. Because this method simulated not only bone morphology but also the bone density of each patient, it allowed for precise and individualized biomechanical analyses of the bone-implant interface under loading. Using these models, the effects of implant angle, length, and rigidity of the provisional restoration on bone-implant interface were investigated biomechanically. They revealed that both longer implants and rigid restorations with reinforcement have the potential to reduce implant micromovements and bone stress; however, the rigidity of restoration has a more significant effect on these parameters.

Acknowledgments

The authors reported no conflicts of interest related to this study.

References

1. Brånemark PI. Osseointegration and its experimental background. J Prosthet Dent 1983;50:399–410.
2. Brånemark PI, Zarb GA, Albrektsson T, eds. Tissue-Integrated Prostheses: Osseointegration in Clinical Dentistry. Chicago: Quintessence, 1985.
3. Albrektsson T, Jansson T, Lekholm U. Osseointegrated dental implants. Dent Clin North Am 1986;30:151–174.
4. Saito H, Tomotake Y, Watanabe M, Nagao D, Ishida Y, Ichikawa T. Survival of immediate implant restoration: A retrospective study through 9-year-observation. J Prosthodont Res 2011;55:141–145.
5. Chiapasco M, Gatti C, Rossi E, Haefliger W, Markwalder TH. Implant-retained mandibular overdentures with immediate loading. A retrospective multicenter study on 226 consecutive cases. Clin Oral Implants Res 1997;8:48–57.
6. Schnitman PA, Wöhrle PS, Rubenstein JE, DaSilva JD, Wang NH. Ten-year results for Brånemark implants immediately loaded with fixed prostheses at implant placement. Int J Oral Maxillofac Implants 1997;12:495–503.
7. Tarnow DP, Emtiaz S, Classi A. Immediate loading of threaded implants at stage 1 surgery in edentulous arches: Ten consecutive case reports with 1- to 5-year data. Int J Oral Maxillofac Implants 1997;12:319–324.
8. Piattelli A, Corigliano M, Scarano A, Quaranta M. Bone reactions to early occlusal loading of two-stage titanium plasma-sprayed implants: A pilot study in monkeys. Int J Periodontics Restorative Dent 1997;17:162–169.
9. Corso M, Sirota C, Fiorellini J, Rasool F, Szmukler-Moncler S, Weber HP. Clinical and radiographic evaluation of early loaded free-standing dental implants with various coatings in beagle dogs. J Prosthet Dent 1999;82:428–435.

10. Szmukler-Moncler S, Piattelli A, Favero GA, Dubruille JH. Considerations preliminary to the application of early and immediate loading protocols in dental implantology. Clin Oral Implants Res 2000;11:12–25.
11. Chiapasco M. Early and immediate restoration and loading of implants in completely edentulous patients. Int J Oral Maxillofac Implants 2004;19(suppl):76–91.
12. Zeren KJ. Minimally invasive extraction and immediate implant placement: The preservation of esthetics. Int J Periodontics Restorative Dent 2006;26:171–181.
13. Molly L. Bone density and primary stability in implant therapy. Clin Oral Implants Res 2006;17(suppl 2):124–135.
14. Buser D, Mericske-Stern R, Bernard JP, et al. Long-term evaluation of non-submerged ITI implants. Part 1: 8-year life table analysis of a prospective multi-center study with 2359 implants. Clin Oral Implants Res 1997;8:161–172.
15. Parel SM, Phillips WR. A risk assessment treatment planning protocol for the four implant immediately loaded maxilla: Preliminary findings. J Prosthet Dent 2011;106:359–366.
16. Brunski JB, Moccia AF, Pollack SR, Korostoff E, Trachtenberg DI. The influence of functional use of endosseous dental implants on the tissue-implant interface. I. Histological aspects. J Dent Res 1979;58:1953–1969.
17. Cameron H, MacNab I, Pilliar R. Porous surfaced Vitallium staples. S Afr J Surg 1972;10:63–70.
18. Cameron HU, Pilliar RM, MacNab I. The effect of movement on the bonding of porous metal to bone. J Biomed Mater Res 1973; 7:301–311.
19. Pilliar RM, Lee JM, Maniatopoulos C. Observations on the effect of movement on bone ingrowth into porous-surfaced implants. Clin Orthop Relat Res 1986:108–113.
20. Brunski JB. Biomechanical factors affecting the bone-dental implant interface. Clin Mater 1992;10:153–201.
21. Szmukler-Moncler S, Salama H, Reingewirtz Y, Dubruille JH. Timing of loading and effect of micromotion on bone-dental implant interface: Review of experimental literature. J Biomed Mater Res 1998;43:192–203.
22. Degidi M, Gehrke P, Spanel A, Piattelli A. Syncrystallization: A technique for temporization of immediately loaded implants with metal-reinforced acrylic resin restorations. Clin Implant Dent Relat Res 2006;8:123–134.
23. Kawahara H, Kawahara D, Hayakawa M, Tamai Y, Kuremoto T, Matsuda S. Osseointegration under immediate loading: Biomechanical stress-strain and bone formation–resorption. Implant Dent 2003;12:61–68.
24. Guan H, van Staden R, Loo YC, Johnson N, Ivanovski S, Meredith N. Influence of bone and dental implant parameters on stress distribution in the mandible: A finite element study. Int J Oral Maxillofac Implants 2009;24:866–876.
25. Guan H, van Staden R, Loo YC, Johnson N, Ivanovski S, Meredith N. Evaluation of multiple implant-bone parameters on stress characteristics in the mandible under traumatic loading conditions. Int J Oral Maxillofac Implants 2010;25:461–472.
26. Baggi L, Cappelloni I, Di Girolamo M, Maceri F, Vairo G. The influence of implant diameter and length on stress distribution of osseointegrated implants related to crestal bone geometry: A three-dimensional finite element analysis. J Prosthet Dent 2008; 100:422–431.
27. Bevilacqua M, Tealdo T, Menini M, et al. The influence of cantilever length and implant inclination on stress distribution in maxillary implant-supported fixed dentures. J Prosthet Dent 2011; 105:5–13.
28. Zarone F, Apicella A, Nicolais L, Aversa R, Sorrentino R. Mandibular flexure and stress build-up in mandibular full-arch fixed prostheses supported by osseointegrated implants. Clin Oral Implants Res 2003;14:103–114.
29. Eto M, Wakabayashi N, Ohyama T. Finite element analysis of deflections in major connectors for maxillary RPDs. Int J Prosthodont 2002;15:433–438.
30. Wada S, Wakabayashi N, Tanaka T, Ohyama T. Influence of abutment selection in maxillary Kennedy Class II RPD on elastic stress distribution in oral mucosa: An FEM study. J Prosthodont 2006; 15:89–94.
31. Wakabayashi N, Ona M, Suzuki T, Igarashi Y. Nonlinear finite element analyses: Advances and challenges in dental applications. J Dent 2008;36:463–471.
32. Takanashi T, Shimamura I, Sakurai K. Influence of width and depth of palatal vault on rigidity of palatal strap: A finite element study. J Prosthodont Res 2009;53:95–100.
33. Baggi L, Cappelloni I, Maceri F, Vairo G. Stress-based performance evaluation of osseointegrated dental implants by finite-element simulation. Simul Model Pract Theory 2008;16:971–987.
34. Wu JC, Chen CS, Yip SW, Hsu ML. Stress distribution and micromotion analyses of immediately loaded implants of varying lengths in the mandible and fibular bone grafts: A three-dimensional finite element analysis. Int J Oral Maxillofac Implants 2012;27:e77–e84.
35. Eskitascioglu G, Usumez A, Sevimay M, Soykan E, Unsal E. The influence of occlusal loading location on stresses transferred to implant-supported prostheses and supporting bone: A three-dimensional finite element study. J Prosthet Dent 2004; 91:144–150.
36. Bessho M, Ohnishi I, Matsuyama J, Matsumoto T, Imai K, Nakamura K. Prediction of strength and strain of the proximal femur by a CT-based finite element method. J Biomech 2007;40: 1745–1753.
37. Ren LM, Arahira T, Todo M, Yoshikawa H, Myoui A. Biomechanical evaluation of porous bioactive ceramics after implantation: Micro CT-based three-dimensional finite element analysis. J Mater Sci Mater Med 2012;23:463–472.
38. Ishikawa M, Nakai T, Sakamoto T, Hirose Y, Ochi M. Three-dimensional finite element analysis of the mandible around immediate loading implants. Jpn Soc Oral Implantol 2012;25 (special issue):300.
39. Qian L, Todo M, Morita Y, Matsushita Y, Koyano K. Deformation analysis of the periodontium considering the viscoelasticity of the periodontal ligament. Dent Mater 2009;25:1285–1292.
40. Kimura K, Fukase Y, Makino M, Masaki C, Nakamoto T, Hosokawa R. Three-dimensional finite element analysis of fixed complete-arch prostheses supported by 4 immediate-loaded implants in the completely edentulous maxilla using clinical computerized tomography data. J Oral Implantol 2011;37: 96–105.
41. Huang H-L, Fuh L-J, Ko C-C, Hsu J-T, Chen C-C. Biomechanical effects of a maxillary implant in the augmented sinus: A three-dimensional finite element analysis. Int J Oral Maxillofac Implants 2009;24:455–462.
42. O'Mahony A, Bowles Q, Woolsey G, Robinson SJ, Spencer P. Stress distribution in the single-unit osseointegrated dental implant: Finite element analyses of axial and off-axial loading. Implant Dent 2000;9:207–218.
43. Begg T, Geerts GA, Gryzagoridis J. Stress patterns around distal angled implants in the all-on-four concept configuration. Int J Oral Maxillofac Implants 2009;24:663–671.